CRYSTAL ORIENTATION DEPENDENCE OF CRACK GROWTH AND CRACK-TIP DEFORMATION IN IRON–3 WT.% SI SINGLE-CRYSTAL THIN PLATES

SỰ PHỤ THUỘC CỦA HƯỚNG TINH THỂ ĐỐI VỚI SỰ PHÁT TRIỂN VẾT NỨT VÀ BIẾN DẠNG TẠI ĐẦU VẾT NỨT TRONG CÁC TẤM MỎNG ĐƠN TINH THỂ IRON–3 WT.% SI

Huynh Thanh Thuong*, Bui Van Huu
Can Tho University
**Email: thanhthuong@ctu.edu.vn*

ABSTRACT

The crack growth behaviour of an iron–3 wt.% silicon single-crystal thin plate was investigated for two different crack orientations, namely $(10\bar{1})[010]$ *and* $(010)[\bar{1}01]$*. The results show that ductile crack growth occurs in both crack orientations under the present testing conditions. However, a pronounced difference in crack-tip deformation behaviour was observed between the two orientations. The crack orientation* $(10\bar{1})[010]$ *exhibits a significantly larger crack-tip opening angle (CTOA) than the (010)[101] orientation. Extensive slip activity was observed in both cases, while more severe slip localisation and pronounced crack-tip blunting were identified for the* $(10\bar{1})[010]$ *orientation. These findings indicate that the slip behaviour in the vicinity of the crack tip plays a dominant role in governing the orientation-dependent crack growth behaviour of Fe–3 wt.% Si single crystals.*

Keywords: *Crack Growth; Crystal Orientation; Single Crystal; BCC Iron.*

TÓM TẮT

Hành vi phát triển vết nứt của tấm mỏng đơn tinh thể sắt – 3% khối lượng silic đã được nghiên cứu đối với hai định hướng vết nứt khác nhau, cụ thể là $(10\bar{1})[010]$ *và* $(010)[\bar{1}01]$*. Kết quả cho thấy sự phát triển vết nứt dẻo xảy ra ở cả hai định hướng vết nứt trong điều kiện thí nghiệm hiện tại. Tuy nhiên, sự khác biệt rõ rệt về hành vi biến dạng tại đầu vết nứt đã được quan sát giữa hai định hướng này. Định hướng vết nứt* $(10\bar{1})[010]$ *thể hiện góc mở đầu vết nứt (CTOA) lớn hơn đáng kể so với định hướng (010)[101]. Hoạt động trượt (slip) diễn ra mạnh mẽ trong cả hai trường hợp, trong khi sự tập trung trượt nghiêm trọng hơn và hiện tượng tù hóa đầu vết nứt rõ rệt hơn được ghi nhận đối với định hướng* $(10\bar{1})[010]$*. Những kết quả này cho thấy hành vi trượt trong vùng lân cận đầu vết nứt đóng vai trò chi phối đối với sự phụ thuộc của quá trình phát triển vết nứt theo định hướng tinh thể trong đơn tinh thể Fe–3 wt.% Si.*

Từ khóa: *Phát triển vết nứt; Định hướng tinh thể; Đơn tinh thể; Sắt BCC.*

1. INTRODUCTION

Fracture toughness is strongly governed by the fracture mechanisms operating within the process zone near the crack tip, where intense stress concentration and localised plastic deformation occur. When the process zone is confined within a single grain, the fracture behaviour is particularly sensitive to crystallographic orientation. Consequently, the orientation of the crack plane and the crack growth direction play a decisive role in determining the dominant fracture mechanisms and crack-propagation behaviour [1-4]. For this reason, investigating the slip behaviour and deformation processes at the crack tip during crack growth has attracted significant attention in fracture mechanics research [5-7].

In practical engineering applications, most metallic materials possess polycrystalline microstructures. However, the presence of grain boundaries introduces additional complexity, as grain-boundary interactions can obscure the intrinsic relationship between crystallography and crack-growth behaviour. To isolate and clarify the fundamental mechanisms governing crack propagation, single-crystalline materials are frequently employed. In particular, single-crystal Fe–Si alloys exhibit relatively high yield strength and are free of grain-boundary effects, making them an ideal model system for studying crack-tip deformation and fracture mechanisms under well-controlled crystallographic conditions [3, 5, 8, 9].

Previous studies have demonstrated that crack orientation strongly influences the fracture behaviour of Fe–Si single crystals, particularly at the brittle–ductile transition at room temperature. Two representative crack orientations, $(001)[\bar{1}10]$ and $(1\bar{1}0)[001]$, have been extensively examined. It has been reported that the $(001)[\bar{1}10]$ orientation exhibits pronounced sensitivity to loading rate, whereas the $(1\bar{1}0)[001]$ orientation shows comparatively stable fracture behaviour over a wide range of loading conditions [1, 10]. These findings indicate that crystallographic orientation governs not only crack propagation paths but also the underlying deformation mechanisms at the crack tip.

Further evidence of orientation-dependent fracture behaviour has been provided by Skogsrud et al. [2], who observed significant dislocation emission and crack-tip blunting without crack growth in a (101)[101] cantilever specimen. In contrast, cleavage-dominated fracture with minimal blunting was reported for the (100)[011] orientation. Similarly, Paul et al. [3] demonstrated that crack-tip blunting is strongly dependent on the crack plane orientation and is controlled by dislocation activity, including twin formation and phase transformation at the crack tip. These studies collectively emphasise that crystallographic orientation dictates the competition between slip-driven plasticity and cleavage-driven fracture.

Despite these advances, a comprehensive understanding of how crack orientation influences crack growth behaviour in thin single-crystal plates remains limited, particularly regarding the associated slip behaviour near the crack tip. Such knowledge is essential not only for advancing fundamental fracture mechanics but also for guiding texture design strategies in Fe–Si-based engineering materials.

In this study, the crack growth behaviour of two distinct crack orientations in an iron–3 wt.% silicon single-crystal thin plate is systematically compared. Particular attention is paid to slip behaviour at the advancing crack tip to clarify the role of crystallographic orientation in governing crack propagation mechanisms. The findings of this work are expected to provide valuable insights into orientation-dependent fracture processes and to contribute to the development of ☞

microstructural and texture-control strategies to improve crack resistance in Fe–Si alloys.

2. EXPERIMENTAL PROCEDURE

Figure 1 schematically illustrates the specimen geometry and crystallographic orientations. Three rectangular specimens, denoted as A1, B1 [11], and B2 [11], were prepared from Fe–3 wt.% Si single crystals with a (101) surface. The gauge dimensions of the specimens were 90 × 30 × 0.18 mm. Specimens were fabricated by electrical discharge machining (EDM). The yield strength (σY) of specimens A and B measured along the [010] and [10$\bar{1}$] directions was 290 MPa [8] and 357 MPa [12], respectively.

A circular hole with a diameter of 0.5 mm was introduced at the center of each specimen by micro-drilling. Subsequently, a through-notch with a length of 1.0 mm and a width of 0.1 mm was introduced by EDM. A fatigue pre-crack was then induced at the notch root under stress-controlled cyclic loading. The total pre-crack lengths (2a) of specimens A1, B1, and B2 were 1.87, 1.64, and 1.98 mm, respectively.

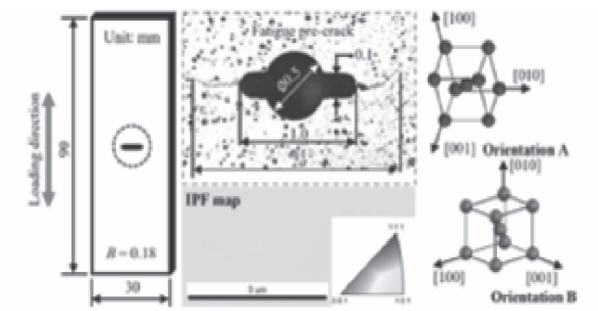

Figure 1. Specimen geometry and crystallographic orientation. The notch and fatigue pre-crack configuration is indicated by the broken-line square. The specimen thickness (B) is 0.18 mm. The IPF map reveals the orientation of the specimen surface.

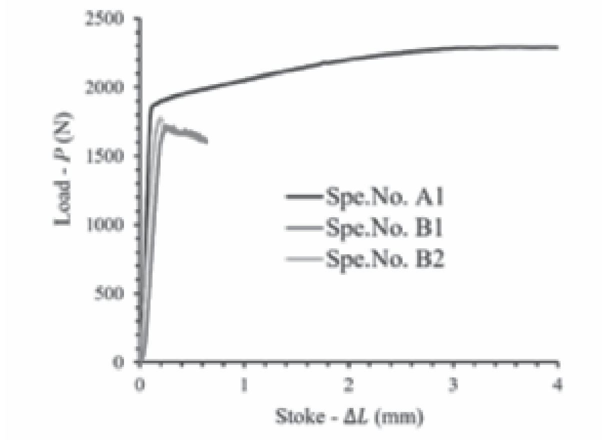

Figure 2. Plots of stroke versus load of the specimens.

Crack growth tests were conducted under displacement-controlled uniaxial tension in air at room temperature using an electro-hydraulic testing machine. A constant crosshead speed of 0.0017 mm/s was applied throughout the tests. The crack growth process was continuously recorded using a video recorder coupled with an optical microscope (KEYENCE VHX-900F). During the tests, the applied load P and the crosshead displacement ΔL were simultaneously recorded. The corresponding ΔL–P curves for specimens A1, B1, and B2 are presented in Fig. 2.

In the crack growth experiments, short crack growth tests were performed for specimens A1 and B1, whereas specimen B1 fractured completely during testing. The unloading process was not recorded. After testing, the topographies of the specimen side surfaces were examined using scanning electron microscopy (SEM) at an accelerating voltage of 15 kV. It should be noted that the fracture tests of specimens B1 and B2 were conducted in a previous study [11]. To facilitate a direct comparison of crack growth behaviour across different crack orientations, the crack growth results for these specimens are revisited in the present work, and their microscopic features are further analysed in greater detail.

3. RESULTS AND DISCUSSION

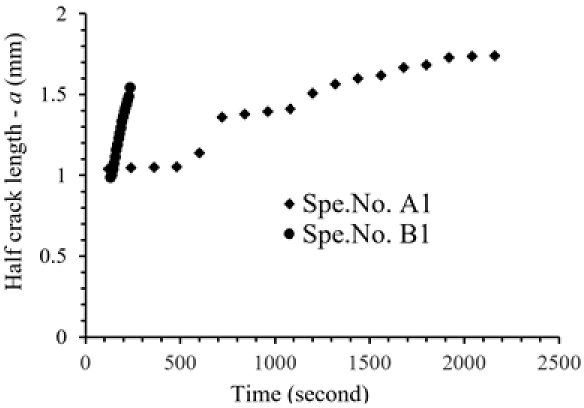

Figure 3. Half crack length a as a function of time.

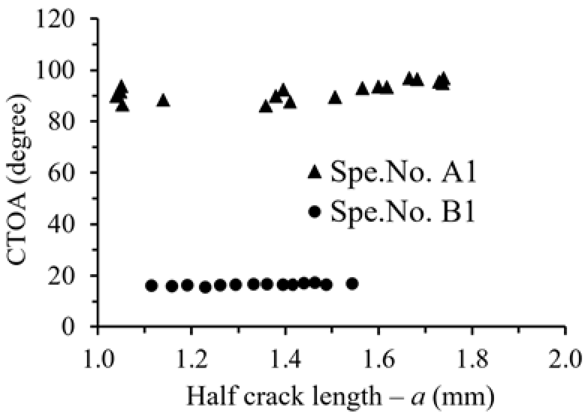

Figure 4. Plots of CTOA versus half crack length a.

Figure 3 shows the evolution of half crack length, a, as a function of time for specimens A1 and B1. In both specimens, stable crack growth was observed throughout the recorded stages. The half-crack length increased approximately linearly with time in both cases; however, the crack growth rate in specimen B1 was significantly higher than that in specimen A1. It should be noted that specimen B1 eventually fractured completely during the crack growth test. Therefore, the crack length data presented in Fig. 3 correspond only to the early stage of crack growth, which is associated with Mode I crack propagation. The later stage of crack growth, corresponding to Mode II propagation, was not recorded for specimen B1.

In contrast, the crack growth test for specimen A1 was intentionally interrupted when the total crack length reached 2a = 4 mm, after which the specimen was unloaded. The interruption was necessary because significant specimen buckling occurred during crack extension.

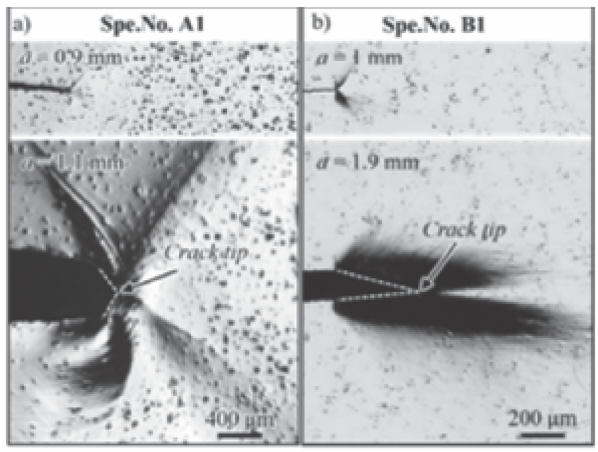

Figure 5. a) and b) show the optical images of the crack growth process of Spe.No.A1 and B1, respectively. The dark regions around the crack wake, where the reflection of light illumination was scarce due to specimen necking, can be seen.

Figure 4 presents the crack tip opening angle (CTOA) as a function of half crack length a. For specimen B1 [11], the CTOA values shown correspond exclusively to the Mode I crack growth regime. A slight increase in CTOA with increasing crack length was observed. In comparison, specimen A1 exhibits substantially higher CTOA values over the measured crack length range. This marked difference indicates a pronounced contrast in crack-tip deformation behaviour between the two crack orientations. ☞

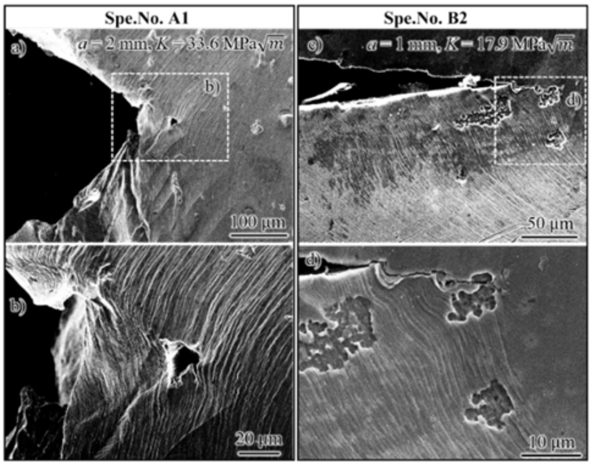

Figure 6. SEM images of the side surfaces of specimen A1 and B2.

Figure 5 presents optical images captured around the crack tip during crack growth in specimens A1 and B1. In each case, the time-dependent crack extension is clearly observed; the upper images correspond to the early stage of crack growth, whereas the lower images represent the later stage. In Fig. 5(b), dark regions are observed in the crack wake due to insufficient light reflection, which is attributed to specimen necking, as reported in previous studies [8]. In contrast, Fig. 5(a) shows specimen buckling at the later stage of crack extension. This buckling is believed to alter light reflection conditions, leading to the appearance of dark regions around the crack.

Figure 6 shows the cracks propagating on the right-hand side of the notch, together with slip traces observed on the side surfaces of specimens A1 and B2. Severe slip activity is evident in specimen A1. A detailed analysis of the slip lines observed in specimen B2 has been reported elsewhere [8], [9]. Figure 6(b) presents a magnified secondary electron image of the region near the crack tip in specimen A1, where pronounced slip activity and significant crack-tip blunting are clearly observed.

For the crack orientation $(010)[\bar{1}01]$, it has been previously suggested that the cleavage plane {001} does not contribute to the crack growth process [9]. Therefore, the influence of the {001} cleavage plane is not considered in the present discussion. Instead, attention is focused on the role of slip behaviour during crack propagation and its influence on crack growth characteristics for the two crack orientations examined.

Specimen A1 corresponds to the crack orientation $(10\bar{1})[010]$, in which no slip systems are activated along the thickness direction [12]. This implies that the in-plane deformation is unaffected mainly by out-of-plane deformation. Furthermore, the inclined slip systems $(1\bar{1}2)[\bar{1}11]$ and $(\bar{1}12)[\bar{1}1\bar{1}]$ are oriented along the hard anti-twinning direction, as indicated by atomistic simulations [1], [4], [13]. In the absence of grain boundary effects, it is therefore speculated that once dislocations are emitted from the crack tip, they readily move away from the crack tip under the applied stress. As a consequence, the shielding effect provided by emitted dislocations diminishes, and the formation of a stable maximum stress field ahead of the crack tip becomes difficult because the dislocations are transported away from the crack front. The emission of complete dislocations at the crack front results in large plastic deformation concentrated on the crack-tip surfaces rather than in the region ahead of the crack [14]. This behaviour leads to pronounced crack-tip blunting and an extremely large crack-tip opening angle (CTOA), as observed in Figure 5 and 6.

In contrast, the crack orientation $(010)[\bar{1}01]$ exhibits more complex slip activity. Out-of-plane deformation, such as necking, reported in previous studies [8], [11], occurs on the $(112)[111]$ and $(\bar{1}\bar{1}2)[\bar{1}\bar{1}1]$ slip systems, or via twinning on the oblique {112}⟨111⟩ planes [15], ahead of the crack tip. These deformation modes significantly influence the in-plane deformation during crack growth. Specifically, the regions ahead of the advancing crack tip are predominantly under plane stress conditions [16], where out-of-plane deformation first initiates on the side surfaces and subsequently propagates into the interior of the specimen. As a result, in-plane deformation is likely obstructed by out-of-plane deformation. Consequently, dislocations emitted from the crack tip on inclined {112}⟨111⟩ slip systems interact with dislocations originating from pre-existing sources on oblique {112}⟨111⟩ slip systems. Such interactions impede the motion of emitted dislocations away from the crack tip, thereby influencing the crack growth behaviour.

Despite the valuable insights provided by the present study, several limitations should be acknowledged. First, the investigation is limited to single-crystal Fe–3 wt.% Si thin plates, and the transferability of the results to polycrystalline materials remains to be clarified. In addition, the crack growth behaviour is mainly interpreted qualitatively based on experimental observations.

From an engineering perspective, the present findings also have broader implications beyond single-crystal systems. A rigorous quantitative analysis, including resolved shear stress and Schmid factor evaluation for each slip system, is not included in the present study. This is because the current work focuses on direct experimental observation of crack growth behaviour. Nevertheless, such quantitative analysis would provide deeper insight into the role of crystallographic orientation and will be systematically addressed in future studies. Future work will focus on incorporating such quantitative approaches and extending the analysis to textured polycrystalline materials.

Although the present study focuses on single-crystal materials, the findings provide important fundamental insights into orientation-dependent deformation mechanisms. In polycrystalline materials, similar mechanisms may operate locally within individual grains, and the overall crack growth behaviour is expected to be influenced by crystallographic texture. Therefore, controlling texture in polycrystalline Fe–Si alloys may offer an effective strategy for improving crack resistance.

5. CONCLUSIONS

The crack growth behaviour of Fe–3 wt.% Si single-crystal thin plates was systematically investigated with a focus on the influence of crystallographic crack orientation. Stable crack growth was observed in both examined orientations; however, a pronounced difference in crack growth rate and crack-tip deformation behaviour was observed. The crack orientation $(10\bar{1})[010]$ exhibited significantly larger crack tip opening angles (CTOA), which were associated with extensive slip activity and pronounced crack-tip blunting. In contrast, the crack orientation $(010)[\bar{1}01]$ showed relatively minor CTOA values and faster crack propagation, reflecting more constrained crack-tip plasticity. These differences were interpreted in terms of orientation-dependent slip activation and the interaction between in-plane and out-of-plane deformation near the crack tip. The results demonstrate that crystallographic orientation plays a critical role in governing crack growth mechanisms by controlling slip behaviour and shielding the crack tip. This study provides fundamental insights into orientation-dependent fracture behaviour in Fe–Si alloys and lays the foundation for future texture-controlled material design to improve crack resistance.❖

☞

References:

[1]. A. Spielmannova, M. Landa, A. Machova, P. Haušild, P. Lejček, "*Influence of crack orientation on the ductile–brittle behavior in Fe–3 wt.% Si single crystals*". Materials Characterization 58 (2007) 892–900.

[2]. J. Skogsrud, C. Thaulow, "*Effect of crystallographic orientation on nanomechanical modelling of an iron single crystal cracked cantilever beam*". Materials Science and Engineering: A 685 (2017) 274–283.

[3]. S.K. Paul, S. Kumar, S. Tarafder, "*Orientation-dependent crack-tip blunting and crack propagation in a single crystal BCC iron*". Bulletin of Materials Science 41 (2018) 1–6.

[4]. A. Spielmannová, A. Machová, P. Hora, "*Crack Orientation versus Ductile-Brittle Behavior in 3D Atomistic Simulations*". Materials Science Forum 567–568 (2008) 61–64.

[5]. Y. Takahashi, M. Tanaka, K. Higashida, H. Noguchi, "*High-voltage electron-microscopic observation of cyclic slip behavior around a fatigue crack tip in an iron alloy*". Scripta Materialia 60 (2009) 717–720.

[6]. S. Rawat, A. Alankar, "*Atomistic analyses of fracture in α, β and lamellar α - β Ti single crystals*". Journal of the Mechanics and Physics of Solids 177 (2023).

[7]. L. Chang, T. Kitamura, C.Y. Zhou, "*Atomic simulation of the orientation effects on crack tip behavior in titanium single crystal*". Theoretical and Applied Fracture Mechanics 110 (2020) 102791.

[8]. T.T. Huynh, M. Koyama, Y. Takahashi, S. Hamada, K. Tsuzaki, H. Noguchi, "*Plastic deformation sequence and strain gradient characteristics of hydrogen-induced delayed crack propagation in single-crystalline Fe–Si alloy*". Scripta Materialia 178 (2020) 99–103.

[9]. T.T. Huynh, S. Hamada, K. Tsuzaki, H. Noguchi, "*Roles of Hydrogen and Plastic Strain Distribution on Delayed Crack Growth in Single-crystalline Fe–Si alloy*". Materials Science and Engineering A 803 (2021) 140703.

[10]. M. Landa, A. Machová, Z. Převorovský, J. Červ, J. Adámek, "*Crack growth in single crystals of α-iron (3 wt.% Si)*". Czechoslovak Journal of Physics 48 (1998) 1589–1606.

[11]. T. Thuong Huynh, S. Hamada, K. Tsuzaki, H. Noguchi, "*Microscopic examination of striation spacing during ductile crack growth in Fe-3wt%Si single-crystalline thin plates in air and hydrogen*". Materials Science and Engineering: A 802 (2021) 140652.

[12]. Y. Takahashi, M. Tanaka, K. Higashida, K. Yamaguchi, H. Noguchi, "*An intrinsic effect of hydrogen on cyclic slip deformation around a {1 1 0} fatigue crack in Fe–3.2 wt.% Si alloy*". Acta Materialia 58 (2010) 1972–1981.

[13]. A. Spielmannová, A. Machová, P. Hora, "*Crack-induced stress, dislocations and acoustic emission by 3-D atomistic simulations in bcc iron*". Acta Materialia 57 (2009) 4065–4073.

[14]. S.P. Lynch, "*Hydrogen embrittlement (HE) phenomena and mechanisms*". Stress Corrosion Cracking: Theory and Practice (2011) 90–130.

[15]. A. Spielmannová, A. Machová, P. Hora, "*Crack orientation versus ductile-brittle behavior in 3D atomistic simulations*". Materials Science Forum, Trans Tech Publ, 2008: pp. 61–64.

[16]. G.T. Hahn, A.R. Rosenfield, "*Local yielding and extension of a crack under plane stress*". Acta Metallurgica 13 (1965) 293–306.